120018582_PRE_11_01_R1_121002_spi

POLYMER REACTION ENGINEERING
Vol. 11, No. 1, pp. 5–20, 2003

An Atomistic Investigation of Solubility and Diffusion of Ethylene in Polyethylene Confined in a Pore[#]

M. Laso,[1,2,*] N. Jimeno,[1] and M. Müller[3]

[1]Department of Chemical Engineering, ETSII, UPM, José Gutiérrez Abascal, Madrid, Spain
[2]Institut für Polymere, and [3]Department of Computer Science, ETH Zürich, Zürich, Switzerland

ABSTRACT

The solubility and diffusivity of ethylene in a polymer-filled nanopore is investigated. The goal is to ascertain whether the thermodynamic and transport properties of the ethylene-polyethylene system are influenced by the confinement in the nanopore. The nanopore is representative of the smallest pores present in current supported polyethylene catalysts.

[#]An earlier version of this paper was presented at ECOREP II, 2nd European Conference on Reaction Engineering of Polyolefins, Lyon, France, July 1–4, 2002.
[*]Correspondence: M. Laso, Department of Chemical Engineering, ETSII, UPM, José Gutiérrez Abacal, 2 E-28006 Madrid, Spain; E-mail: laso@diquima.upm.es.

DOI: 10.1081/PRE-120018582 1054-3414 (Print); 1532-2408 (Online)

Advanced modeling techniques are used to generate a single atomistic polyethylene chain confined in the pore. Subsequently, Monte Carlo and Molecular techniques are employed to determine thermodynamic (phase equilibrium) and transport properties of the ethylene-polyethylene system for two different pore sizes. For the smallest pore, both types of properties differ from their values in macroscopic bulk systems. Such differences are shown to be a consequence of confinement in the nanopore and can be of relevance in catalyst design and in mesoscopic and macroscopic modeling of heterogenous polyolefin catalysis.

AQ1

INTRODUCTION

Modeling heterogeneous supported catalysts for polyeolefin synthesis is a challenging area in which great advances have been made in the last few years (Ferrero and Chiovetta, 1987a,b). Recent models have achieved a considerable degree of realism through the incorporation of a wide range of transport and kinetic phenomena in a consistent way (Estenoz and Chiovetta, 2001; Hutchinson et al., 1992).

The increasing detail of such meso- and microscopic models makes it necessary to deal with thermodynamic and transport phenomena at very small spatial scales. Although the complexity (fractal geometries, coexistence and multicomponent equilibrium and diffusion of monomer, oligomers and polymer, actual kinetics on active sites, etc.) of existing supported catalysts puts them out of reach of atomistically detailed simulations, the very small time and length scales at which diffusion, phase equilibria and reaction (incorporation of monomers to growing polymer chains) take place pose some fundamental questions as to the applicability of macroscopic continuum descriptions of these phenomena.

The present investigation attempts to quantitatively answer the question of the applicability of macroscopic descriptions to 1) solubility (phase equilibrium) and 2) diffusion in very confined geometries. To that end, atomistic modeling techniques are applied to an idealized pore in which a polymer chain (polyethylene, PE) and monomer (ethylene, Et) are present. Although modeling the reaction (i.e. chain growth at the expense of monomer) at an active site in the pore could be treated on a semiempirical basis (Leach, 1996), it has been deliberately left out in order to focus on the thermodynamic and transport aspects of the problem. The main goal of the present work was therefore to determine monomer availability at the reaction site as controlled both by diffusivity and solubility.

MODEL SYSTEMS FOR ATOMISTIC ETHYLENE/POLYETHYLENE STRUCTURES CONFINED IN A PORE

In all work reported in the following, the pore was modeled as a cylindrical cavity of total depth $H + (D/2)$ consisting of a cylinder of diameter D and height H capped by a semisphere of diameter D. Two pore sizes were considered: $D = 3$ nm and $D = 1.5$ nm (see Figure 1). In both cases, $H \approx 5$ nm (average over the Monte Carlo run; see below). These dimensions are thought to be representative of typical structures of supported catalysts where active catalyst sites are located (Dickson et al., 1996). F1

The model system consisted of a single molecule of linear polyethylene of length 1246 backbone carbon atoms in the pore with $D = 3$ nm and 311

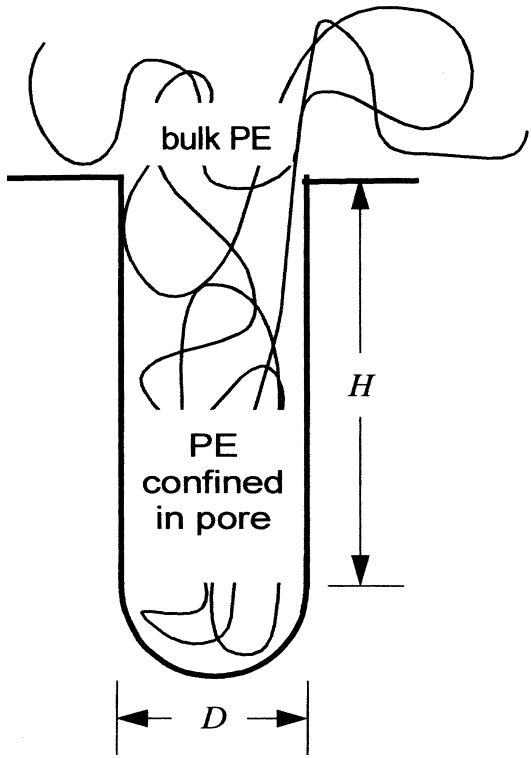

Figure 1. Schematic of pore. A single chain of PE is grown in the pore. The bulk is represented by a separate cubic simulation box under three-dimensional boundary conditions.

backbone carbon atoms in the pore with $D = 1.5$ nm, while the number of ethylene molecules fluctuated in the Monte Carlo (MC) and was fixed in the Molecular Dynamics (MD) calculations reported below. Polyethylene was modeled using a united-atom representation for both methylene and methyl end groups, nonbonded interactions being described by a Lennard-Jones potential:

$$V_{ij}^{LJ}(r) = 4\varepsilon\left[\left(\frac{\sigma_{ij}}{r_{ij}}\right)^{12} - \left(\frac{\sigma_{ij}}{r_{ij}}\right)^{6}\right] \tag{1}$$

with r_{ij} being the scalar minimum image distance between sites i and j. Along a PE chain, all pairs of sites separated by more than three bonds along the chain and all intermolecular sites interact via the Lennard-Jones pair potential. Potential tails are cut at 1.45 σ_{PE} and brought smoothly down to zero at 2.33 σ_{PE} using a quintic spline.

In the generation of the starting structure, bond lengths were kept constant, whereas bond angles were assumed to fluctuate around an equilibrium angle θ_0 of 112° subject to the Van der Ploeg and Berendsen bending potential (Van der Ploeg and Berendsen, 1982) of the form:

$$V_{bending}(\theta) = (1/2)K_\theta(\theta - \theta_0)^2 \tag{2}$$

with K_θ 482.23 kJ/mol. Associated with each dihedral angle ϕ was also a torsional potential of the form (Ryckaert and Bellemans, 1975):

$$\begin{aligned} V_{torsion}(\phi) \;=\; & c_0 + c_1\cos(\phi) + c_2(\cos(\phi))^2 + c_3(\cos(\phi))^3 \\ & + c_4(\cos(\phi))^4 + c_5(\cos(\phi))^5 \end{aligned} \tag{3}$$

with $c_0 = 9.28$, $c_1 = 12.16$, $c_2 = -13.123$, $c_3 = -3.06$, $c_4 = 26.25$, and $c_5 = -31.51$ in kJ/mol. In Molecular Dynamics calculations, C–C bonds were constrained by a standard harmonic potential (Brooks et al., 1988). Ethylene was also represented in the united atom mode following (Cornell et al., 1995). Pore walls were represented by a Catlow potential frequently used in zeolite modeling (Raj et al., 1999).

MODEL SYSTEMS AND TECHNIQUES

Solubility of Ethylene in Polyethylene Structures Confined in a Pore

Solubility is the first of the two key factors influencing permeability of ethylene in PE. Its direct measurement in nanopores is still beyond the

reach of available experimental techniques. It is therefore natural that current modeling work assumes the macroscopic value of Et/PE solubility to be valid at all scales down to the finest structures of the catalyst.

Molecular modeling techniques, in particular Monte Carlo, offer a way to computationally test the validity of this assumption. To this end, we performed Gibbs ensemble simulations (De Pablo et al., 1992a; Laso et al., 1992), in which thermodynamic equilibrium was established between a pure ethylene box and the PE-filled pore depicted in Figure 1 at 353 K and 10 bar.

The first type of moves in a Gibbs ensemble simulation, namely *NvT* moves, were achieved by simple Metropolis moves for ethylene (both in the pure ethylene box and in the pore). Efficient configurational sampling for the polymer in *NvT* moves was much more challenging, since neither Continuum Configurational Bias (De Pablo et al., 1992b; Rosenbluth and Rosenbluth, 1953; Siepmann and Frenkel, 1992) nor End-Bridging Monte Carlo (Mavrantzas et al., 1999) were effective in the restricted space of the pore. The Extended Concerted Rotation (ECROT) of Leontidis et al. (1994) however proved to be very efficient at performing local rearrangements of polymer segments. ECROT moves were supplemented with a combination of single angle Metropolis, reptation and flip moves. Although not as efficient as ECROT, these moves are known to act as a ''lubricant'' in MC calculations and improve overall sampling when used in conjuntion with larger scale moves like ECROT or End-Bridging. The overall strategy for *NvT* moves consisted thus in 85% ECROT, 5% single angle Metropolis, 5% reptation and 5% flip moves.

Another main hurdle in the simulation of such highly constrained systems was the generation of the starting configuration for the MC run. The very recent (Müller et al., 2001) and highly efficient (García Pascua et al., 2002) initial guess generator Polypack was used to densely pack the PE chain in the pore. Polypack is one of the most flexible and efficient polymer structure generators and is based on a geometric optimization approach. The polymer chain packing problem is cast as a geometric optimization taks which is then solved by heuristic search algorithms. It can generate dense packings of long chains for virtually any polymer structure, no matter how complex its architecture.

The ability of Polypack to produce acceptable, dense initial structures of long chains in the very confined space of a pore is very remarkable. (C_{1246} in the $D=3$ nm pore and C_{311} in the $D=1.5$ nm pore). Although these initial structures had high intramolecular non-bonded energies due to a few overlaps, these overlaps were not severe and were rapidly eliminated by the ECROT algorithm during the equilibration phase (5×10^6 steps). After equilibrating the confined PE structures, a full Gibbs ensemble simulation was initiated, in which cycles of 1000 *NvT* moves

(configurational sampling), 1 NpT move (volume fluctuation) and 10000 μvT moves (ethylene exchange between boxes) were executed. For the small pore, 3.3×10^5 cycles and for the large pore 5.8×10^6 cycles were performed.

Volume fluctuations in the ethylene box were achieved in the usual way (scaling of cubic box edge). Coupled volume fluctuations in the pore were carried out by changing H and leaving D constant, which is consistent with the assumption that the pore is an undeformable cavity and volume fluctuations can only take place in the axial direction. This procedure is tantamount to placing a movable lid or piston over the pore. Volume fluctuations correspond to displacements of this piston. During NpT moves, the lid was endowed with the same potential as the pore walls.

In view of the small size of the ethylene molecule, simple brute-force insertions of ethylene molecules into both boxes (pure Et box and PE-filled pore) were used for particle exchange and resulted in sufficiently high acceptance ratio 1.8% and 3.4% for the small and large box, respectively. A block analysis showed that the efficiency of the suite of MC moves was amply sufficient to generate decorrelated PE structures after every 800 cycles in the small pore and every 2200 cycles in the large pore.

All computations were carried out in a simple parallel fashion on individual processors of a 24-CPU Beowulf Linux cluster composed of inexpensive Pentium III processors. The complete MC simulation of the small system ($D = 1.5$ nm pore), including the equilibration phase, took 26 hours, whereas the $D = 3$ nm pore required 510 hours (accumulated wall clock over all processors).

Figures 2 and 3 are graphical representations of typical configurations produced during the MC calculation. They give an idea of the smallness of the pore and the high degree of confinement of the ethylene/polyethylene system. F2/F3

Diffusivity of Ethylene in Polyethylene Structures Confined in a Pore

Diffusivity being a dynamic or transport property, it is natural to use a dynamic method such as a MD to investigate it. Fully decorrelated configurations from the MC calculations (previous paragraphs) were used as initial configurations (García Pascua et al., 2002) for MD simulations. We employed standard MD using the velocity Verlet method (Swope et al., 1982) with $\Delta t = 0.45$ fs. Periodic rescaling was used to maintain

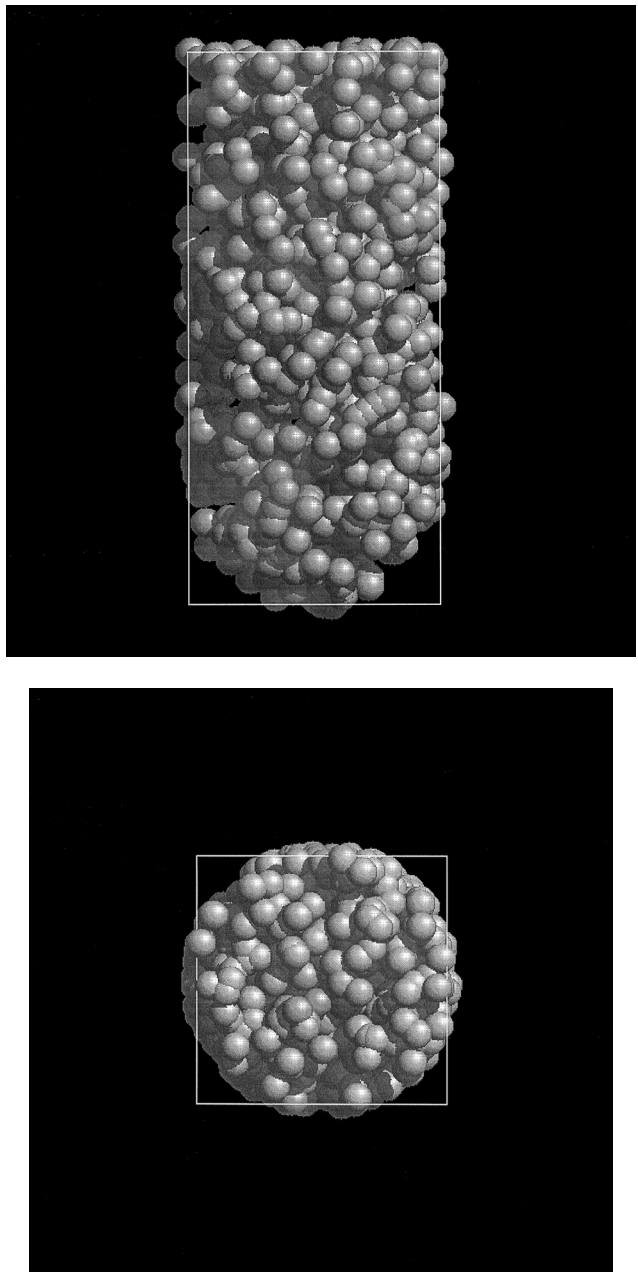

Figure 2. Side (a) and top (b) views of C_{1246} in large pore ($D = 3$ nm, $H \approx 5$ nm).

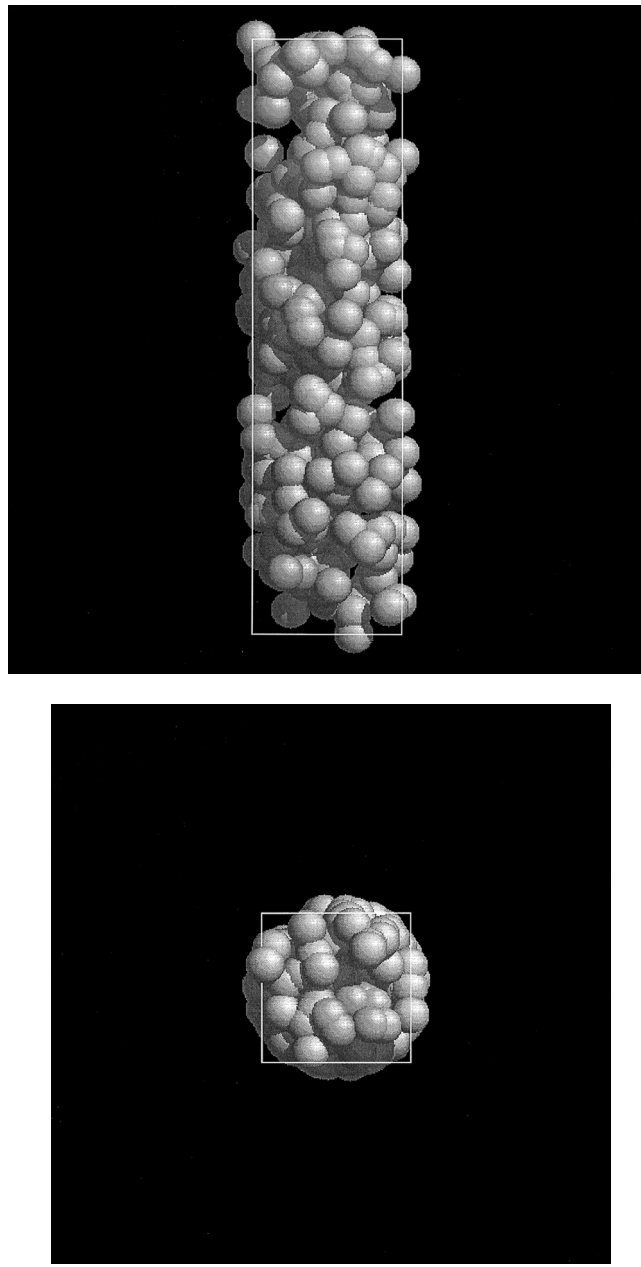

Figure 3. Side (a) and top (b) views of C_{311} in the small pore ($D = 1$ nm, $H \approx 5$ nm).

temperature at the set value (Allen and Tildesley, 1987). In addition to the PE chain, a number of ethylene molecules were also present in the system. The number of ethylene molecules was taken to be the nearest integer to the average number of ethylene molecules present in the corresponding MC calculation. Independent MD runs were started from individual MC configurations and executed on different processors. For each initial structure, trajectories for all ethylene molecules were stored. Results were subsequently pooled over all structures and trajectories in order to reduce statistical uncertainty in the diffusivity.

RESULTS

Solubility of Ethylene in Polyethylene Confined in a Pore

The main results of the Gibbs ensemble calculations are density and composition of both phases. The average density in the pore was found to be 738 ± 0.2 kg/m^3 (one standard deviation of the mean) with typical fluctuations of 40 kg/m^3 (one standard deviation) for the large pore and 671 ± 0.3 kg/m^3 with typical fluctuations of 35 kg/m^3 (one standard deviation) for the small pore. An independent calculation of the same molecular model of PE in the bulk (three-dimensional periodic boundary conditions) yielded 801 ± 02 kg/m^3 for pure PE (García Pascua et al., 2002). The differences between pure bulk and confined systems are therefore highly significant and are a consequence of the confinement: although quite flexible, PE chains have a certain rigidity and therefore feel the presence of the pore walls when the pore size approaches the order of magnitude of the chain persistence length. The effect is more marked in the smaller pore, since the diameter of the pore is barely sufficient to allow the PE chain to turn around within it. As a matter of fact, the PE chain adopts conformations with high torsional and non-bonded potential energy. These conformations are rich in *gauche* defects and have a correspondingly higher proportion of ''hairpin'' turns than chains in the bulk.

Unlike in the work of Baschnagel et al. (2000), the density profile of monomeric residues of the PE chain across the pore does not display any obvious maximum in the center of the pore. The PE chain fills the pore quite uniformly in the axial direction as well. On the other hand, the inability of PE to fill the pore at the same density as in the bulk implies that additional volume must be available for the ethylene solute compared with a bulk system. This effect is also evident in the relatively high acceptance ratios for molecule insertions in the Gibbs ensemble calculation.

Solubility of ethylene was found to be 0.012 ± 0.001 gEt/gPE in the large pore and 0.019 ± 0.001 gEt/gPE in the small pore, which is higher than experimental values, than EOS calculations and also higher than bulk simulations at the same conditions (0.004 ± 0.0003 gEt/gPE). It therefore seems that ethylene solubility is noticeably enhanced in confined geometries. Since the ethylene molecule is much smaller than the pore diameter, solubility is enhanced through an energetic mechanism (greater available volume) and is not hindered by an entropic mechanism, as could be the case in very small pores of a size comparable to that of the ethylene molecule. The consequence is an overall enrichment effect with respect to the bulk. Enhanced ethylene concentration close to active sites will almost certainly have a positive influence on polymerization reaction rate, although this point warrants a careful investigation.

Equilibrium thermodynamic properties of highly confined PE are therefore markedly different from those of bulk (''macroscopic'') PE. The more so, the smaller the pore diameter. Although the system studied is an idealization of real PE confined in real catalyst pores, the results obtained are highly suggestive that at the very small scale, where monomer incorporation to the chain takes place, PE bears little resemblance to the bulk material.

Diffusivity of Ethylene in Polyethylene Confined in a Pore

Analyzing the MD runs in confined geometry in order to obtain the diffusivity of ethylene in PE is a rather difficult task for two reasons. First, the slow progression of ethylene molecules through the PE matrix makes it necessary to run extremely long calculations. Secondly, ethylene diffusion takes place in a restricted volume and therefore cannot achieve an Einsteinian diffusion regime due the presence of walls. Current sophisticated methods for the evaluation of diffusivity (Gusev and Suter, 1993; Gusev et al., 1994) are unfortunately not applicable in confined geometries, since they rely on the diffusion through an infinite domain (periodically infinite as in periodic boundary conditions).

Here we have followed an alternative approach based on tagging diffusant molecules and monitoring their positions (and through averaging, their concentration) as they follow deterministic trajectories through the fully elastic PE matrix. In this way, concentration of ethylene through the pore can be mapped at different times. Thanks to the axial symmetry, data can also be accumulated by projecting on the radial-axial plane, with a significant improvement in the quality of the statistics.

Nevertheless the method is subject to strong statistical noise. The results obtained below were obtained from a set of 146 independent MD trajectories, each of them 1.1×10^7 steps long. Typically, around a dozen molecules of ethylene diffused in each structure. Unlike for small penetrants (Gusev et al., 1994), full polymer chain flexibility was found to be an absolute requirement for ethylene to diffuse.

There is a subtle point worth discussing in the evaluation of the concentration profiles. One of our goals is to answer the question of whether diffusion in a confined polymer obeys classical macroscopic laws. In an periodically infinite simulation box, the determination of the diffusivity according to (Gusev et al., 1994), although expensive in terms of computation, is rather straightforward, since that method is actually using the well known solution of a diffusion problem in an infinite 3D domain. The situation in a finite domain like the pore is quite different, since no analytical solution with which to compare the evolution of the concentration is available. Answering the question posed above requires that we compare the time dependent concentration field obtained from the MD calculation with time dependent concentration fields obtained by solving the macroscopic diffusion equation in the same confined domain and with a given value of the diffusivity. The answer to the question is positive (i.e. the behavior is in agreement with macroscopic conservation and constitutive laws) if it is possible to find a numerical value for the diffusivity for which the solution of the continuum diffusion equation matches the results of the MD calculations.

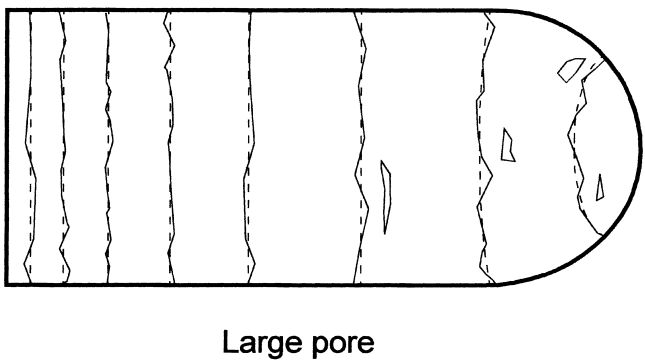

Figure 4. Contour plot of ethylene concentration in the large pore on a plane that contains the pore axis and at $t = 10^{-9}$ s. Isolines correspond to equally spaced concetration values. Solid lines are results of MD calculation. Dashed lines represent the numerical solution of the classical diffusion equation in the pore for $D_{Et,PE} = 7.2 \times 10^{-9}$ m^2/s.

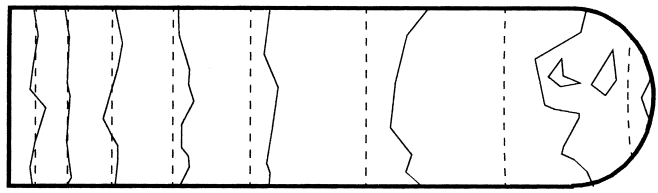

Figure 5. Contour plot of ethylene concentration in the small pore on a plane that contains the pore axis and at $t = 5 \times 10^{-10}$ s. Isolines correspond to equally spaced concentration values. Solid lines are results of MD calculation. Dashed lines represent the numerical solution of the classical diffusion equation in the pore for $D_{Et,\,PE} = 12.5 \times 10^{-9}$ m^2/s.

According to this strategy, we have solved the unsteady diffusion equation in the axisymmetric geometry defined in Figure 1 using finite elements techniques. Different values of the diffusivity were tried until an optimum match to the concentration field from the MD calculation was obtained.

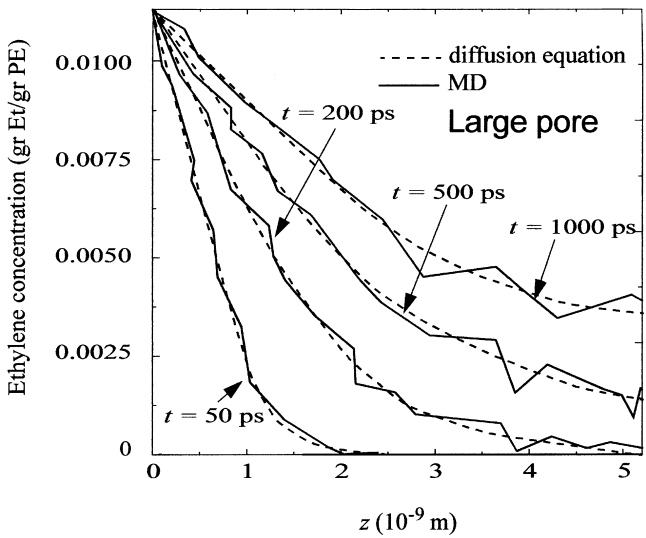

Figure 6. Ethylene concentration profiles along the pore axis for the large pore at four different times. Solid lines are results of MD calculation. Dashed lines are numerical solution of the diffusion equation for $D_{Et,\,PE} = 7.2 \times 10^{-9}$ m^2/s.

For the large pore (Figures 4 and 5), the solution of the unsteady diffusion equation with $D_{Et,\ PE}$ 7.2×10^{-9} m^2/s is found to match the MD results within the statistical uncertainty of the latter (small closed contour lines in Figure 4 are due to statistical noise). Even close to the bottom of the pore, where the diffusion problem is more strongly two dimensional and the contour lines have the greatest curvature, the agreement is complete. We can therefore conclude that the diffusive behaviour of ethylene in a PE-filled pore of about 3 nm diameter is well described by the macroscopic diffusion equation. On the other hand, the value of $D_{Et,\ PE}$ is higher than in bulk PE, most probably as a consequence of the lower density of PE in the pore and the associated enhanced available volume for diffusion.

For the small pore the best match between MD and macroscopic calculations was found for a value of $D_{Et,\ PE} = 12.5 \times 10^{-9}$ m^2/s. The quality of this optimum match, however, is poor (Figures 6 and 7). Although it is possible to match the MD results in specific regions of the pore (e.g. close to the pore entry in Figure 6, where the isolines overlap), it is not possible to simultaneously extend the match to the whole spatial and temporal domains. Ethylene concentrations deeper in the pore are systematically higher than what the macroscopic diffusion equation

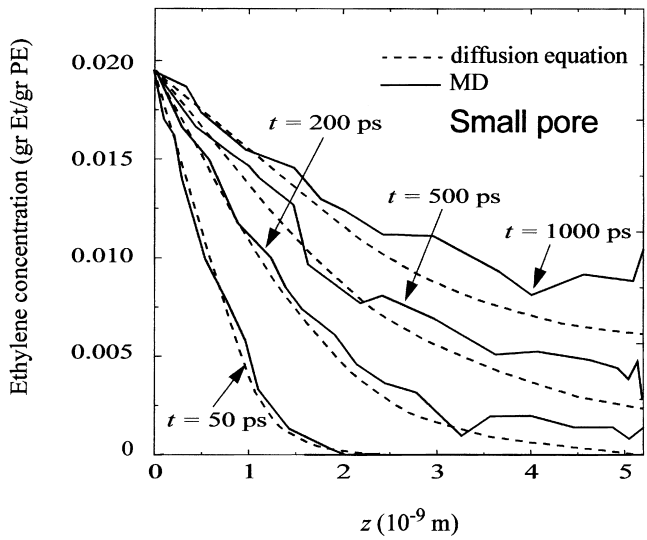

Figure 7. Ethylene concentration profiles along the pore axis for the small pore at four different times. Solid lines are results of MD calculation. Dashed lines are numerical solution of the diffusion equation for $D_{Et,\ PE} = 12.5 \times 10^{-9}$ m^2/s.

predicts. This effect is more pronounced at longer times (Figure 7). As we have seen, the 1.5 nm pore is small enough to severely constrain the conformation of the PE chain and prevent its efficient filling of the pore. As a consequence, ethylene diffuses faster than in the bulk and in a way that cannot be reconciled with the macroscopic diffusion equation with a constant value of $D_{Et,\ PE}$. It is of course possible to maintain the macroscopic formalism by assuming a phenomenological, position dependent $D_{Et,\ PE}$. This would of course come at the price that there is no *a priori* macroscopic way of predicting that dependence.

As far as ethylene diffusivity is concerned, the 1.5 nm pore seems to be truly microscopic and the macroscopic description breaks down.

CONCLUSIONS

The atomistic investigation of solubility and diffusivity of ethylene in a nanopore filled with polyethylene by means of MC and MC techniques strongly suggests that thermodynamic and transport properties of a confined system differ markedly from their counterparts in the bulk.

Polyethylene density in the pore is significantly lower than in the bulk as a consequence of the restricted space available. Hairpin chain turns and bonds in *gauche* state occur with higher probability than in the bulk. These high-energy conformations are required for the PE chain to be able to fit in the available pore volume.

Solubility of ethylene is predicted to be enhanced due to the lower density of the PE matrix and the ensuing greater available volume for insertion. The same mechanism is responsible for the enhanced value of the diffusivity as compared with the bulk value. Ethylene transport is seen to obey the macroscopic diffusion equation in the large pore. In the small pore however, the behavior of ethylene is quantitatively and qualitatively different from behavior in the bulk and cannot be described by the macroscopic diffusion equation with constant diffusivity. As far as ethylene transport in PE is concerned, a 1 nm pore behaves as a microsocopic object, whereas a pore of 3 nm diameter can already be described by standard macroscopic conservation and constitutive laws. Molecular modeling techniques offer a way to investigate the former type of system.

The observed deviations in solubility and diffusivity of ethylene in polyethylene confined in a nanopore are such that they would increase the amount of monomer available for reaction (incorporation into a growing polyethylene chain) should the pore contain an active catalytic site. This observation may be of some relevance for the design and modeling of more efficient supported catalysts.

ACKNOWLEDGMENTS

This work was partially supported by CICYT grant MAT 1999-0972. Very fruitful discussions with Prof. P. Herodek are gratefully acknowledged.

REFERENCES AQ3

Allen, M. P., Tildesley, D.J. (1987). *Computer Simulation of Liquids.* Oxford University Press.

Baschnagel, J., Mischler, C., Binder, K. (2000). Dynamics of confined polymer melts: recent Monte Carlo simulation results. In: Frick, B., Zorn, R., Büttner, H., Eds.; *Proceedings of the International Workshop on Dynamics in Confinement.* Vol. 10, Pr 7, May.

Brooks, C.K. III, Karplus, M., Pettitt, B.M. (1988). Proteins: a theoretical perspective of dynamics, structure and thermodynamics. *Advances in Chemical Physics.* Vol. LXXI. John Wiley & Sons.

Cornell, W.D., Cieplak, P., Bayly, C.I., Gould, I.R., Merz, K.M. Jr., Ferguson, D.M., Spellmeyer, D.C., Fox, T., Caldwell, J.W., Kollman, P.A. (1995). A second generation force field for the simulation of proteins, nucleic acids, and organic molecules. *J. Am. Chem. Soc.* 117:5179.

De Pablo, J.J., Laso, M., Suter, U.W. (1992a). Estimation of the chemical potential of chain molecules by simulation. *J. Chem. Phys.* 96:6157.

De Pablo, J.J., Laso, M., Suter, U.W. (1992b). Simulation of polyethylene above and below the melting point. *J. Chem. Phys.* 96:2395.

Dickson, R.M., Norris, D.J., Tzeng, Y.-L., Moerner, W.E. (1996). Three-dimensional imaging of single molecules solvated in pores of poly(acrylamide) gels. *Science* 274:966.

Estenoz, D., Chiovetta, M. (2001). Olefin polymerization using supported metallocene catalysts: a process representation scheme and mathematical model. *J. Appl. Pol. Sci.* 85:285.

Ferrero, M., Chiovetta, M. (1987a). Catalysts fragmentation during propylene polymerization: Part I. The effects of grain size and structure. *Pol. Eng. Sci.* 27:1436.

Ferrero, M., Chiovetta, M. (1987b). Catalysts fragmentation during propylene polymerization: Part I. Microparticle diffusion and reaction effects. *Pol. Eng. Sci.* 27:1447.

García Pascua, O., Ahumada, O., Müller, M., Laso, M. (2002). The effect of AQ4 the initial guess generator on molecular mechanics calculations. *Mol. Sim. in press.*

Gusev, A.A., Suter, U.W. (1993). A model for transport of diatomic molecules through elastic solids. *J. Comput.-Aided Mater. Des.* 1:63.

Gusev, A.A., Müller-Plathé, F., van Gunsteren, W.F., Suter, U.W. (1994). Dynamics of small molecules in bulk polymers. Special volume on ''*Atomistic Modeling of Physical Properties of Polymers*'' of *Adv. Polym. Sci.* 116:273.

Hutchinson, R., Chen, C., Ray, W. (1992). Polymerization of olefins through heterogeneous catalysis. X. Modeling of particle growth and morphology. *J. Appl. Pol. Sci.* 44:1389.

Laso, M., De Pablo, J.J., Suter, U.W. (1992). Simulation of phase equilibria for chain molecules. *J. Chem. Phys.* 97:2817.

Leach, A.R. (1996). *Molecular Modeling. Principles and Applications.* Longman.

Leontidis, E., De Pablo, J.J., Laso, M., Suter, U.W. (1994). A critical evaluation of novel algorithms for the off-lattice Monte Carlo simulation of condensed polymer phases. *Adv. Polym. Sci.* 116:283. ''*Atomistic Modelling of Physical Properties*'', Chapter VIII, Springer Verlag.

Mavrantzas, V.G., Boone, T.D., Zervopoulou, E., Theodorou, D.N. (1999). End-bridging Monte Carlo: an ultrafast algorithm for atomistic simulation of condensed phases of long polymer chains. *Macromolecules* 32:5072.

Müller, M., Nievergelt, J., Santos, S., Suter, U.W. (2001). A novel geometric embedding algorithm for efficiently generating dense polymer structures. *J. Chem. Phys.* 114:9764.

Raj, N., Sastre, G., Catlow, C.R.A. (1999). Diffusion of octane in silicalite: a molecular dynamics study. *J. Phys. Chem. B* 103:11007.

Rosenbluth, M.N., Rosenbluth, A.W. (1953). Equations of state calculations by fast computing machines. *J. Chem. Phys.* 21:1087.

Ryckaert, J.P., Bellemans, A. (1975). Molecular dynamics of liquid n-butane near its boiling point. *Chem. Phys. Lett.* 30:123.

Siepmann, J.I., Frenkel, D. (1992). Configurational bias Monte Carlo: a new sampling scheme for flexible chains. *Mol. Phys.* 59.

Swope, W.C., Anderson, H.C., Berens, P.H., Wilson, K.R. (1982). A computer simulation method for the calculation of equilibrium constants for the formation of physical clusters of molecules: application to small water clusters. *J. Chem. Phys.* 76:637.

Van der Ploeg, P., Berendsen, H.J.C. (1982). Molecular dynamics simulation of a bilayer membrane. *J. Chem. Phys.* 76:3271.

Received July 22, 2002
Accepted September 23, 2002